(http://www.sciencedirect.com/science/journal/00224596)

ISSN: 0022-4596

Journal of Solid State Chemistry

› Supports Open Access (http://www.elsevier.com/journals/journal-of-solid-state-chemistry/0022-4596/open-access-options)

Editor-in-Chief: M.G. Kanatzidis (https://www.journals.elsevier.com:443/journal-of-solid-state-chemistry/editorial-board/mg-kanatzidis)

› View Editorial Board (https://www.journals.elsevier.com:443/journal-of-solid-state-chemistry/editorial-board)

Submit Your Paper

View Articles (http://www.sciencedirect.com/science/journal/00224596)

Guide for Authors

Abstracting/ Indexing (http://www.elsevier.com/journals/journal-of-solid-state-chemistry/0022-4596/abstracting-indexing)

Journal of Solid State Chemistry 221 (2015) 79–84

Contents lists available at ScienceDirect

Journal of Solid State Chemistry

journal homepage: www.elsevier.com/locate/jssc

Mercury (I) nitroprusside: A 2D structure supported on homometallic interactions

H. Osiry [a], A. Cano [a], L. Reguera [b], A.A. Lemus-Santana [a], E. Reguera [a,*]

[a] Centro de Investigación en Ciencia Aplicada y Tecnología Avanzada, Unidad Legaria, Instituto Politécnico Nacional, México
[b] Facultad de Química, Universidad de La Habana, Cuba

ARTICLE INFO

Article history:
Received 15 June 2014
Received in revised form
15 September 2014
Accepted 21 September 2014
Available online 30 September 2014

Keywords:
Hg–Hg dimer
Homometallic interaction
Mercury nitroprusside
Layered solid

ABSTRACT

The pentacyanonitrosylferrate complex anion, $[Fe(CN)_5NO]^{2-}$, forms an insoluble solid with Hg(I) ion, of formula unit $Hg_2[Fe(CN)_5NO]\cdot 2H_2O$, whose crystal structure and related properties are unknown. This contribution reports the preparation of that compound by the precipitation method and its structural study from X-ray powder patterns complemented with spectroscopic information from IR, Raman, and UV–vis techniques. The crystal structure was solved ab initio and then refined using the Rietveld method. The solid crystallizes with a triclinic unit cell, in the $P-1$ space group, with cell parameters $a=10.1202(12)$, $b=10.1000(13)$, $c=7.4704(11)$ Å; $\alpha=110.664(10)$, $\beta=110.114(10)$, $\gamma=104.724(8)$ °. Within the unit cell, two formula units are accommodated ($Z=2$). It adopts a layered structure related with the coordination of the equatorial CN groups at their N end to the Hg atoms while the axial CN ligand remains unlinked. Within the layers neighboring $Hg_2[Fe(CN)_5NO]$ building units remain linked through four relatively strong Hg–Hg interactions, with an interatomic distance of 2.549(3) Å. The charge donation from the equatorial CN groups through their 5σ orbitals results into an increase for the electron density on the Hg atoms, which strengths the Hg–Hg bond. In the Raman spectrum, that metal–metal bond is detected as a stretching vibration band at 167 cm^{-1}. The available free volume between neighboring layers accommodates two water molecules, which are stabilized within the framework through hydrogen bonds with the N end of the unlinked axial CN group. The removal of these weakly bonded water molecules results in structural disorder for the material 3D framework.

1. Introduction

The coordination chemistry of heavy metals, among them mercury, has received considerable attention in the last decades related with their high toxicity for biological species [1]. Binding of metal ions to the heteroatomic sites of biomolecules is, without doubt, fundamental to explain their physiological effects. The increasing load of mercury in the biosphere, as consequence of anthropogenic activities, has stimulated the interest for the mercury coordination chemistry, including those compounds involving ligands able to form aqueous insoluble mercurial solids [2]. The precipitation reactions provide a means for mercury removal from ground water and liquid industrial wastes.

The metal–metal interactions and their nature are active areas of research in chemistry [3]. In this sense, the Hg–Hg interaction, usually observed in Hg (I) coordination compounds, has played a prototypical role [4]. The dispersive forces between metal centers magnified by relativistic effects explain the nature of such metal–metal bond [4,5]. Charge donating ligands linked to the metals favor a stronger metal–metal bond [6]. The role of donor–acceptor interaction in the stability of the metal–metal bond also contributes to the formation of heterometallic pairs, for instance, in Hg (II) · · · Au (I), Hg (II) · · · Pt (II), and Hg (II) · · · Pt (II) [3,6,7].

The titled compound forms part of a metal salts series of the pentacyanonitrosylferrate complex anion, $[Fe(CN)_5NO]^{2-}$, commonly known as nitroprussides, first documented by Playfair in 1848 [8]. The insoluble members of that series are formed by salts of divalent transition metals (M^{2+} = Mn^{2+}, Fe^{2+}, Co^{2+}, Ni^{2+}, Cu^{2+}, Zn^{2+} and Cd^{2+}) and of Cu(I), Ag(I), Hg(I) and Hg(II). The preparation and characterization of these metal nitroprussides have been studied from 1950s decade [9–14]. The crystal structure and related properties of these solids are known for divalent transition metals (M^{2+}) [15,16], but not for Cu(I), Ag(I), Hg(I) and Hg(II). This contribution reports the synthesis, structure and properties of Hg(I) nitroprusside. In its crystal structure, a relatively strong homometallic interaction between neighboring Hg atoms was identified, which is favored by the charge donation from the equatorial CN ligands. This solid has a 2D structure based on the assembling of $Hg_2[Fe(CN)_5NO]$ blocks through four of such Hg–Hg bonds. The structural study was complemented by

* Corresponding author.
E-mail address: edilso.reguera@gmail.com (E. Reguera).

http://dx.doi.org/10.1016/j.jssc.2014.09.021
0022-4596/

information from IR, Raman and UV–vis spectroscopies, thermogravimetry and adsorption isotherms.

2. Experimental

The material under study was prepared by the precipitation method, from diluted aqueous solutions (1:2 M ratio) of sodium nitroprusside, $Na_2[Fe(CN)_5NO]\cdot 2H_2O$ and mercury (I) nitrate, $Hg(NO_3)\cdot 2H_2O$. These chemicals were Sigma-Aldrich products. The formed precipitate was aged for three days within the mother liqueur, then separated by centrifugation and washed several times with distilled water until to obtain a filtrate free of the involved ligands. The obtained solid was air dried until it had constant weight. IR and Raman spectroscopies confirmed its nature as a metal nitroprusside. According to X-ray fluorescence spectroscopy, the atomic Hg:Fe metals ratio was 2:1. The material hydration degree and thermal stability were evaluated recording thermogravimetric (TG) curves under an N_2 flow.

X-ray powder diffraction (XRD) patterns were recorded in the 5–80°/2θ range, with a scan step of 0.008°, using Cu$K\alpha_1$ radiation in a D8 Advance diffractometer (from Bruker). The unit cell identification was carried out with DICVOL program [17]. The diffraction pattern was decomposed for single and overlapping intensities according to the Le Bail method using pseudo Voigt peak profile function [18]. The structural model to be refined was derived by simulated annealing using EXPO2013 program for structure determination by direct space approaches [19]. The structural model was completed from the analysis of the corresponding electron density Fourier maps. The Rietveld method, implemented in the FullProf program, was used for the crystal structure refinement [20]. In the refinement process, the Fe–C and C–N interatomic distances were constrained to change within the expected values for metal nitroprussides. Preferential orientation was also refined in order to obtain an appropriate pattern fitting. The atomic packing within the unit cell was visualized with the help of Diamond package software [21]. Table 1 summarizes the XRD experimental conditions and the parameters values related with structure solution and refinement.

The stability of the 3D crystal structure on the weakly bonded water molecules removal was evaluated from XRD powders for the hydrated and anhydrous samples, complemented with H_2 adsorption isotherms recorded at 75 K (the local N_2 boiling point).

Table 1
Details of data collection, crystal data and structure refinement for $Hg_2[Fe(CN)_5NO]\cdot 2H_2O$.

Diffractometer	D8 adavnced
Radiation	Cu$K\alpha_1$, Ge monochromator
2θ range (°)	5–80
Step scan (°)	0.008
Count time (s/step)	10
Crystal system	Triclinic
Space group	$P-1$
a (Å)	10.1202(12)
b (Å)	10.1000(13)
c (Å)	7.4704(11)
α (°)	110.664(10)
β (°)	110.114(10)
γ (°)	104.724(8)
V (Å^3)	606.51(13)
Z	2
Number of observations	749
Number of reflections	384
Number of structural parameters refined	68
Number of profile parameters refined	19
Number of distance restrictions	10
R_{exp}	5.483
R_{wp}	7.873
R_B	8.119
S	1.435

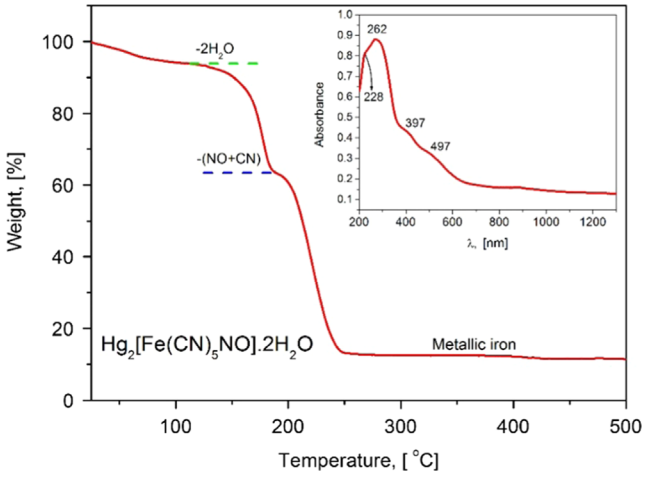

Fig. 1. TG curve and UV–vis spectrum (inset) for $Hg_2[Fe(CN)_5NO]\cdot 2H_2O$.

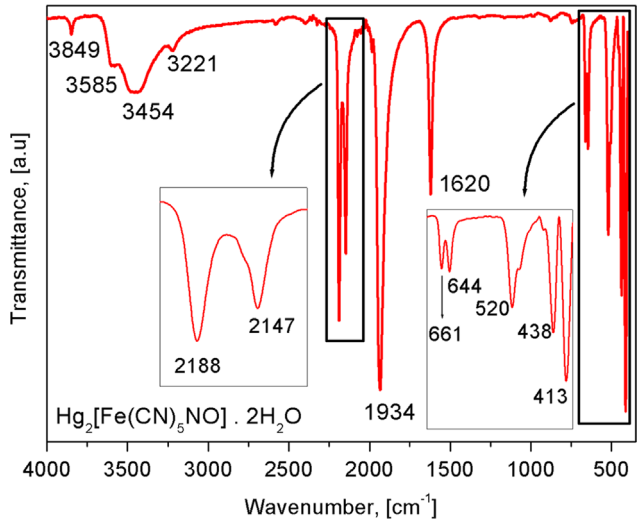

Fig. 2. IR spectrum, recorded by the ATR method, for $Hg_2[Fe(CN)_5NO]\cdot 2H_2O$.

3. Results and discussion

3.1. Characterization of mercury (I) nitroprusside

Fig. 1 shows the TG curve for the material under study. On heating, below 100 °C it loses two water molecules indicating that on the precipitation reaction a dihydrate was formed. The evolution of the two water molecules is followed by a progressive weight loss, which ends at 190 °C. These second thermal effects were ascribed to the evolution of two ligand molecules, NO+CN. From that point, also the remaining four CN groups and the two mercury atoms evolve which results in the formation of metallic iron as final product. The evolved cyanide radicals behave as reducing agent giving C_2N_2 and metallic iron. This is a well-known process during the thermal decomposition of transition metal cyanides [22].

Fig. 2 shows the IR spectrum for the titled compound. The middle spectral region is dominated by the ν(NO) stretching vibration at 1934 cm^{-1} and two ν(CN) bands at 2147 and 2188 cm^{-1}. The appearance of these two ν(CN) bands with a frequency separation of 41 cm^{-1} reveals the existence of both,

bridged and unbridged CN ligands. An analog behavior, with similar frequency separation, is observed for copper (II) nitroprusside dihydrate, which has a layered structure, where the equatorial CN groups are found linked to the copper atom while the axial one remains unlinked [23]. The band at 1620 cm^{-1} corresponds to the bending vibration, δ(HOH), for weakly bonded water molecules. For coordinated water molecules, that vibration is observed about 1600 cm^{-1} [23]. Four ν(OH) stretching vibrations from these weakly water molecules dominate the high frequency spectral region; two of these bands appear unresolved at 3454 cm^{-1}. The presence of these four ν(OH) bands is conclusive clue on the existence of two different types of weakly bonded water molecules. The narrow and weak band at 3849 cm^{-1} was attributed to an overtone, 2ν(NO), of the intense ν(NO) stretching vibration. Below 1000 cm^{-1} five well-resolved absorption bands appear (Fig. 2, inset), at 661, 644, 520, 438 and 413 cm^{-1}, which were ascribed to δ(FeNO), ν(FeN), $\delta(FeCN)_{eq.+ax}$, $\nu(FeC)_{eq,\ A'+A''}$ and $\nu(FeC)_{eq,\ A'}$ vibrations, respectively [24]. The appearance of two unresolved bands for the $\delta(FeCN)_{eq.+ax}$ bending motion at 520 cm^{-1} coincides with the information provided by the ν(CN) stretching concerning the existence of bridged and unbridged CN ligands.

UV–vis spectrum for mercury (I) nitroprusside has limited structural information because the Hg(I) ion ($5d^{10}6s^1$) has no *d–d* transitions, which are sensitive to the metal ion coordination environment. All the absorption bands detected in the recorded spectrum (see Fig. 1, inset) corresponds to metal–ligand electronic charge transfers within the nitroprusside ion. These bands are observed at 262, 397 and 497 nm, and were ascribed to $11e \rightarrow 13e$, $12e \rightarrow 13e$, and $2b_2 \rightarrow 13e$ transitions [25]. The unresolved band at 228 nm was attributed to the $12e \rightarrow 4b_1$ transition.

3.2. Crystal structure

Mercury (I) nitroprusside dihydrate crystallizes in a triclinic unit cell in the $P-1$ space group, with cell parameters: $\boldsymbol{a}=10.1202(12)$, $\boldsymbol{b}=10.1000(13)$, $\boldsymbol{c}=7.4704(11)$ Å; $\boldsymbol{\alpha}=110.664(10)$, $\boldsymbol{\beta}=110.114(10)$, $\boldsymbol{\gamma}=104.724(8)^{\circ}$. The unit cell accommodates two formula units ($Z=2$).

To solve the structure, standard heavy atom and direct methods were initially applied, without success, so a strategy based on global optimization in the direct space by simulating annealing method was adopted. To run EXPO 2013 for structure solution, the unit asymmetric content information was required. It was derived by taking into account the expected molecular geometry. A suitable number of orientations and translations of the whole molecule were automatically generated by the program applying simulated annealing method. The finding of the appropriate structural model was monitored by the matching between experimental and calculated powder diffraction patterns plots, and considering the atomic packing within the unit cell and the correspondence of the calculated model with the *a priori* available structural information from spectroscopic techniques. Finally, the best structural model obtained was refined by the Rietveld method. The O atoms from non-coordinated water molecules were located by difference Fourier synthesis. Fig. 3 shows the experimental, fitted and difference XRD powder patterns. The experimental pattern is properly reproduced by the refined structure even at the highest diffraction angles (see Fig. 3, inset). The obtained merit figures for the fitting are summarized in Table 1. For the crystal structure solution and refinement from powder XRD, in addition to the merit figures, the validity of the derived structural model must be supported by both, its physical meaning and the available *a priori* information from complementary techniques.

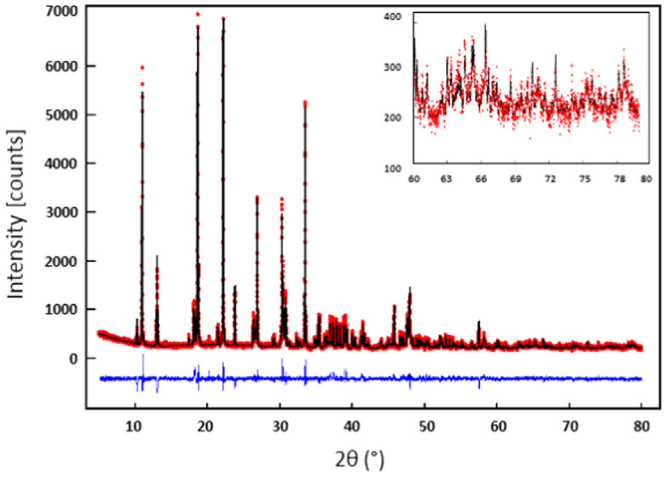

Fig. 3. XRD patterns, experimental, fitted and their difference, for $Hg_2[Fe(CN)_5NO] \cdot 2H_2O$. Inset shows the highest angles region.

Fig. 4 shows the coordination environment for the involved atoms. The coordination environment for the mercury atom is formed by two N ends of CN groups plus the homometallic Hg–Hg interaction. The CN groups for two neighboring Hg atoms have an alternate disposition (Fig. 4), which minimizes the ligand–ligand repulsive interaction and favors the homometallic bond. The axial CN and NO groups remain unlinked, in correspondence with the IR spectrum feature already discussed. The axial CN group stabilizes the two water molecules within the structure through bifurcated hydrogen bonding interactions at the N end, with slightly different N–O distance, which is supported by the observed four IR absorption bands in the 3600–3200 cm^{-1} spectral region, from symmetric and asymmetric ν(OH) stretching vibrations. The two weakly bonded water molecules occupy the available pore volume in the resulting 3D framework. The coordination of equatorial CN groups to the Hg atoms determines the layered structure adopted by the solid (Fig. 5).

The layered structure appears as the 2D assembling of $Hg_2[Fe(CN)_5NO]$ building units through such metal–metal bond (Fig. 6). Neighboring layers are maintained together through dispersive forces to form the 3D crystal structure. Table 2 summarizes the refined atomic positions and temperature and occupation factors derived from the structure Rietveld refinement. Table 3 collects the calculated interatomic distances and bond angles. The Fe–C and $Fe–N_{NO}$ distances are similar to those reported for the series of metal nitroprussides [26–30]. The pseudo-octahedral $[Fe(CN)_5NO]$ unit remains as a practically rigid block during the solid formation. According to the calculated values for the Hg–N distance, which are in the 2.36–2.66 Å range, the Hg atoms have a highly distorted planar coordination environment. These Hg–N interatomic distances are within the expected values for nitroprusside metal salt of heavy metals, e.g. Cd [27]. The weakly bonded water molecules are located at two quite different distances from the donor N atom, particularly, 2.778(3) and 2.830(3) Å (Table 4). This is supported by the frequency difference for the four ν(OH) stretching vibrations, which are observed at 3585, 3454 (doublet) and 3221 cm^{-1} (Fig. 2).

The Hg–Hg interatomic distance, calculated from the refined atomic positions, is relatively short, 2.549(3) Å. In mercury (I) coordination compounds that distance is found in the range 2.5–3.5 Å range [4,31]. The metal–metal bond observed in heavy metals, particularly between closed-shell metal atoms, as already mentioned, is attributed to dispersive forces magnified by relativistic effects. The dispersive forces are enhanced by an increase of the available electron density on the involved atoms. For

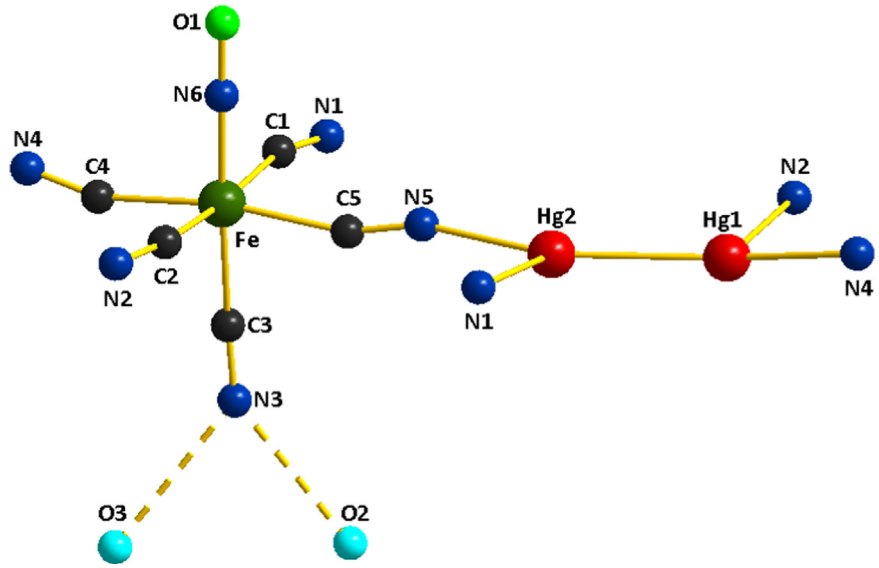

Fig. 4. Coordination environment for the involved atoms in the formula unit $Hg_2[Fe(CN)_5NO]\cdot 2H_2O$.

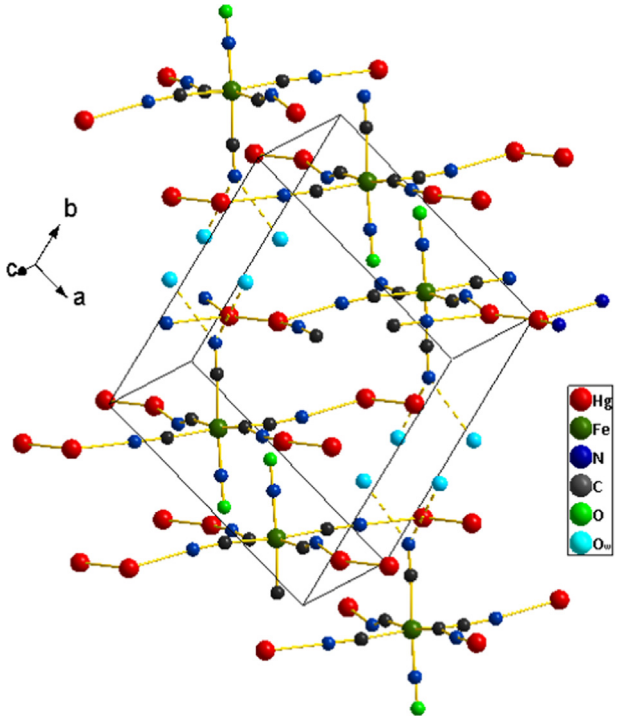

Fig. 5. Atomic packing within the unit cell for $Hg_2[Fe(CN)_5NO]\cdot 2H_2O$.

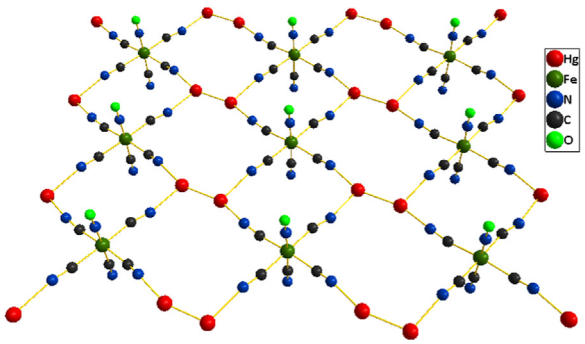

Fig. 6. 2D structure for mercury (I) nitroprusside, formed by the assembling of $Hg_2[Fe(CN)_5NO]$ units by Hg–Hg interactions.

Table 2
Atomic coordinates and equivalent isotropic displacement parameters for $Hg_2[Fe(CN)_5NO]\cdot 2H_2O$.

Atom	Wyck.	*x*	*y*	*z*	*U* (Å^2)
Hg1	2*i*	1.0451 (3)	1.2308 (3)	0.0696 (5)	0.027 (3)
Hg2	2*i*	0.2750 (3)	0.4592 (3)	−0.5702 (5)	0.027 (3)
Fe	2*i*	0.6502 (7)	0.8589 (7)	0.2516 (10)	0.012 (2)
C1	2*i*	0.5196 (3)	0.7377 (3)	0.3264 (3)	0.05 (3)
C2	2*i*	0.7722 (2)	0.9770 (3)	0.1640 (2)	0.05 (3)
C3	2*i*	0.7540 (2)	0.7229 (2)	0.2513 (4)	0.05 (3)
C4	2*i*	0.8141 (2)	1.0086 (15)	0.5467 (13)	0.05 (3)
C5	2*i*	0.4971 (2)	0.7210 (13)	−0.0520 (16)	0.05 (3)
N1	2*i*	0.4329 (11)	0.6406 (3)	0.3263 (4)	0.05 (3)
N2	2*i*	0.8780 (2)	1.0669 (10)	0.1834 (3)	0.05 (3)
N3	2*i*	0.8240 (2)	0.6517 (2)	0.2466 (8)	0.05 (3)
N4	2*i*	0.8342 (16)	1.0939 (11)	0.7121 (12)	0.05 (3)
N5	2*i*	0.4285 (11)	0.5927 (13)	−0.1793 (15)	0.05 (3)
N6	2*i*	0.5509 (6)	0.9655 (6)	0.2403 (8)	0.05 (3)
O1	2*i*	0.4804 (5)	1.0343 (5)	0.2341 (6)	0.05 (3)
O2	2*i*	0.1923 (13)	0.6452 (13)	−0.0382 (17)	0.14 (3)
O3	2*i*	1.1295 (12)	0.6812 (12)	0.4620 (16)	0.14 (3)

instance, the critical temperature within the noble gases increases according to their electron density: 5.19 (He), 44.4 (Ne), 150.66 (Ar), 209.48 (Kr), and 289.73 (Xe) K [32]. The CN ligand has the ability to subtract electron density from the metal bound at the C end (Fe) through a mechanism known as π-back donation. That electron density is located on the most electronegative N atom and partially donated through the 5σ orbital of the CN group to the metal linked at the N end. Such charge redistribution within the –Fe–C ≡ N–Hg – chain results in an increase for the electron density on the Hg atoms. This could explain the relatively strong metal–metal bond assessed through the Hg–Hg distance. The electron density involved in the metal–metal bond, is highly polarizable and from this feature, quite sensible for Raman spectroscopy. In the recorded Raman spectrum an intense peak at 167 cm^{-1} band is observed (Supplementary Information), which was ascribed to the metal–metal stretching band.

The above discussed structural features found for $Hg_2[Fe(CN)_5NO]\cdot 2H_2O$ are unique within the metal nitroprussides series, both by the presence of the metal–metal bond and the appearance of water molecules hydrogen bonded to the N end of the unlinked axial CN group. For that series, a dihydrate of layered (2D) structure is also observed for copper but with the two water

Table 3
Selected bond lengths (Å) and bond angle (°) for Hg_2 $[Fe(CN)_5NO]\cdot 2H_2O$.

Bond distances (Å)			
Hg1[a]–Hg2	2.56(3)	Fe–C5	1.934(11)
Hg1–N2	2.62(4)	Fe–N6	1.653(10)
Hg1[b]–N4	2.361(16)	C1–N1	1.14(4)
Hg2[b]–N1	2.62(5)	C2–N2	1.14(3)
Hg2–N5	2.41(3)	C3–N3	1.131(4)
Fe–C1	1.93(3)	C4–N4	1.139(15)
Fe–C2	1.93(3)	C5–N5	1.133(13)
Fe–C3	1.93(3)	N6–O1	1.12(6)
Fe–C4	1.938(9)		
Bond angles (°)			
C1–Fe–C2	177(2)	C5–Fe–N6	84.5(15)
C1–Fe–C3	87(2)	N2–Hg1–N4[c]	89.4(13)
C1–Fe–C4	96.9(14)	N1–Hg2[b]–N5[b]	101.8(2)
C1–Fe–C5	88.5(16)	Fe–C1–N1	164.8(3)
C1–Fe–N6	91(2)	Fe–C2–N2	157(2)
C2–Fe–C3	95(2)	Fe–C3–N3	173.3(3)
C2–Fe–C4	85.6(13)	Fe–C4–N4	141.8(9)
C2–Fe–C5	89.0(13)	Fe–C5–N5	142.1(10)
C2–Fe–N6	87.1(19)	Fe–N6–O1	177.5(7)
C3–Fe–C4	88.3(14)	Hg1–N2–C2	158(3)
C3–Fe–C5	92.5(17)	Hg1[b]–N4–C4	134.3(11)
C4–Fe–C5	174.6(9)	Hg2[b]–N1–C1	166(4)
C4–Fe–N6	94.9(16)	Hg2–N5–C5	133(2)

[a] $x-1, y-1, z-1$.
[b] $x, y, z+1$.
[c] $x, y, z-1$.

Table 4
Hydrogen bond distances (Å).

D – H · · · A	D · · · A
O2 · · · N3[a]	2.78 (3)
O3 · · · N3	2.83 (3)

[a] $-x+1, -y+1, -z$.

molecules coordinated to the axial positions for the copper atoms [23]. It seems, the observed structure for the mercury coordination compound under study is determined by the possibility of a metal–metal bond formation related to the highly polarizable electron cloud on the mercury atom which determines the strength for the dispersive interactions, with also the contribution of the mentioned relativistic effect.

3.3. *Structural stability on the water molecules removal*

It is well documented that hydrogen bonds can play an important role to maintain packing and stability in coordination compounds [33]. In this sense, according to the TG curve (Fig. 1), the two hydrogen bonded water molecules are easily removed by moderate heating. From 80 °C these water molecules evolve. The XRD patterns recorded for hydrated and heat-treated samples reveal that from a heating of 70 °C structural changes are detected (see Supplementary Information). For the sample heated at 100 °C, the XRD amorphous fraction is remarkable. The volume occupied by the two water molecules is sufficient to accommodate at least a N_2 molecule because it has a kinetic diameter of 4.5 Å [32], but no framework accessibility for nitrogen was detected for anhydrous samples. Hydrogen has a smaller kinetic diameter, 2.9 Å [32], and from such feature, H_2 adsorption isotherms were recorded. The available pore volume for the anhydrous solid is accessible for the hydrogen molecule but the limiting adsorption capacity is 0.43 molecule per cavity (Fig. 7). This value is relatively low for a cavity that in the original solid has a volume sufficient to accommodate

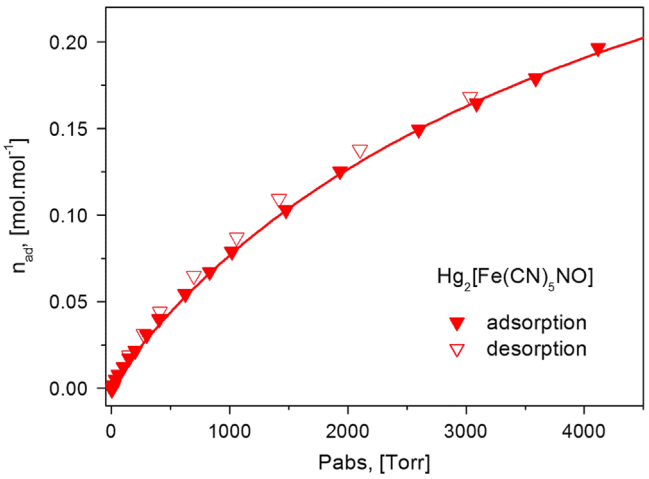

Fig. 7. H_2 adsorption isotherm, recorded at 75 K, for $Hg_2[Fe(CN)_5NO]$.

two water molecules. This suggests that on the removal of the hydrogen bonded water molecules the material porous framework collapses. Such behavior is quite different to that observed for the copper analog, where the removal of the crystal water molecules results in the formation of a 3D crystalline solid of relatively high thermal stability [23].

4. Conclusions

Mercury (I) nitroprusside crystalizes as a dihydrate with a triclinic unit cell in the $P-1$ space group. The four equatorial CN groups are found coordinated to Hg atoms while the axial ligands remain unlinked. This results into a layered structure formed by $Hg_2[Fe(CN)_5NO]$ building block assembled by four homometallic Hg–Hg bonds. The Hg–Hg bond is particularly strong, with an interatomic distance of 2.549(3) Å. Such feature was ascribed to an increase of the electron density on the mercury atoms related to the charge donation from the CN ligand enhanced by charge subtraction from the inner iron atom through the π-back donation effect. An increase in the electron density on the Hg atoms favors the appearance of stronger dispersive forces that contribute to maintain together the two neighboring metals. The two water molecules are stabilized within the solid framework through hydrogen bridges with the N end of the unlinked CN group. When these water molecules are removed, on heating, the material porous framework collapses. Such structural features for this mercury (I) coordination compound are unique within the metal nitroprussides series.

Acknowledgments

This study was partially supported by the CONACyT projects 2011-01-174247, FON.INST./75/2012 and 154626. The authors thank the multiple suggestions from Dr. J. Duque concerning the use of simulated annealing processing of powder XRD data.

Appendix A. Supporting information

Supplementary data associated with this article can be found in the online version at http://dx.doi.org/10.1016/j.jssc.2014.09.021.

References

[1] I. Onyido, A.R. Norris, E. Buncel, Chem. Rev. 104 (2004) 5911.
[2] X. Wang, L. Andrews, Inorg. Chem. 44 (2005) 108.
[3] M. Kim, T.J. Taylor, F.P. Gabbai, J. Am. Chem. Soc. 130 (2008) 6332.
[4] P. Schwerdtfeger, P.D.W. Boyd, S. Brienne, J.S. McFeaters, M. Dolg, M.-S. Liao, W.H.E. Schwarz, Inorg. Chim. Acta 213 (1993) 233–246 (and references therein).
[5] P. Pyykkö, Angew. Chem. Int. Ed. 43 (2004) 4412.
[6] N.L. Draper, R.J. Batchelor, P.M. Aguilar, S. Kroeker, D.B. Leznoff, Inorg. Chem. 43 (2004) 6557.
[7] J.M. López-de-Luzuriaga, M. Monge, M.E. Olmos, D. Pascual, T. Lasanta, Chem. Commun. 47 (2011) 6795–6797.
[8] L. Playfair, Proc. R. Soc. Lond. 5 (1848) 846.
[9] P.G. Salvadeo, Gazz. Chim. Ital. 89 (1959) 2184.
[10] L.A. Gentil, E.J. Baran, P.J. Aymonino, Z. Naturforsch. 23b (1968) 1264.
[11] J.B. Ayres, W.H. Waggoner, J. Inorg. Nucl. Chem. 31 (1969) 2045.
[12] A.N. Garg, P.S. Goel, Inorg. Chem. 10 (1971) 1344.
[13] H. Inoue, H. Iwase, S. Yanagisawa, Inorg. Chim. Acta 7 (1973) 259.
[14] D.B. Brown, Inor. Chem. 14 (1975) 2582.
[15] E. Reguera, A. Dago, A. Gómez, J.F. Bertrán, Polyhedron 15 (1996) 3139 (and references therein).
[16] L. Reguera, J. Balmaseda, C.P. Krap, E. Reguera, J. Phys. Chem. C 112 (2008) 10490 (and references therein).
[17] A. Boultif, D. Louer, J. Appl. Cryst. 24 (1991) (1991) 987.
[18] A. Le Bail, H. Duroy, J.L. Fourquet, Mat. Res. Bull. 23 (1988) 447.
[19] A. Altomare, C. Cuocci, C. Giacovazzo, A. Moliterni, R. Rizzi, EXPO2013, Institute of Crystallography CNR, Bari – Italy, 2013.
[20] J. Rodrígues– Carvajal, Fullprof Suite 2013, Institute Leon Brillouin, Saclay, 2013.
[21] K. Branderbug, H. Putz, Diamond V 3.2, Crystal Impact GbR, Bonn, Germany, 2009.
[22] R. Robinette, R.L. Collins, J. Coord. Chem. 4 (1974) 65.
[23] A. Gómez, J. Rodríguez-Hernández, E. Reguera, J. Chem. Crystallogr. 34 (2004) 893.
[24] A. Benavante, J.A. de Morán, O.E. Piro, E.E. Castellano, P.J. Aymonino, J. Chem. Crystallogr. 27 (1997) 343.
[25] P.T. Manoharan, H.B. Gray, J. Am. Chem. Soc. 87 (1965) 3340.
[26] D.F. Mullica, D.B. Tippin, E.L. Sappenfield, D.H. Leschnitzer, Inorg. Chim. Acta 164 (1989) 99.
[27] D.F. Mullica, D.B. Tippin, E.L. Sappenfield, Inorg. Chim. Acta 174 (1990) 129.
[28] D.F. Mullica, D.B. Tippin, E.L. Sappenfield, J. Cryst. Spectrosc. Res. 21 (1991) 81.
[29] D.F. Mullica, D.B. Tippin, E.L. Sappenfield, J. Coord. Chem. 24 (1991) 83.
[30] D.F. Mullica, D.B. Tippin, E.L. Sappenfield, J. Coord. Chem. 25 (1992) 175.
[31] E. Guzmán-Percástegui, L.N. Zakharov, J.G. Alvarado-Rodríguez, M.E. Carnes, D.W. Johnson, Cryst. Growth Des. 14 (2014) 2087.
[32] D.R. Lide (Ed.), CRC Handbook of Chemistry and Physics, 84th edition,CRC Press, Fl., USA, 2004.
[33] D.F. Li, S. Gao, L.M. Zheng, W.Y. Sun, T. Okamura, N. Ueyama, W.X. Tang, New J. Chem. 26 (2002) 485.